Journal of Microbiological Methods 161 (2019) 63–70

Contents lists available at ScienceDirect

Journal of Microbiological Methods

journal homepage: www.elsevier.com/locate/jmicmeth

Electrochemical detection of food-spoiling bacteria using interdigitated platinum microelectrodes

Olga Fysun[a,b,*,1], Alexander Schmitt[b,c,2], Peter Thomas Auernhammer[a,b,3], Johannes Rauschnabel[b], Horst-Christian Langowski[a,d]

[a] TUM School of Life Sciences Weihenstephan, Technical University of Munich, Freising, Germany
[b] Robert Bosch Packaging Technology GmbH, Waiblingen, Germany
[c] Faculty of Applied Chemistry, Nuremberg Institute of Technology, Nuremberg, Germany
[d] Fraunhofer Institute for Process Engineering and Packaging IVV, Freising, Germany

ARTICLE INFO

Keywords:
Cyclic voltammetry
Interdigitated microelectrodes
Bacillus subtilis ssp. *subtilis*
Paenibacillus polymyxa
Pseudomonas fragi
Bacterial biofilms

ABSTRACT

The fast and non-destructive detection of bacterial attachment on food contact surfaces is important for the prevention of the unwanted formation of biofilms. Biofilms constitute a protected growth mode that allows bacteria to survive even in hostile environments. Therefore, the fast detection of bacterial attachment may be an effective strategy for biofilm control. In this study cyclic voltammetry (CV) was used to detect *Bacillus subtilis* ssp. *subtilis, Paenibacillus polymyxa, Pseudomonas fragi* attachment on interdigitated microelectrodes. The differences in current between the uncolonized sterile microelectrodes and the microelectrodes after bacterial attachment were determined. In addition, the surface coverage of microelectrodes was visualized using microscopy techniques. The results showed that the cyclic voltammetry in combination with interdigitated platinum microelectrodes can be used to detect bacterial biofilms.

1. Introduction

Fast and non-destructive biofilm detection is an important issue for medicine, food safety, and public health. The presence of bacteria can lead to problems such as infection propagation and biocorrosion of surfaces among many others (Cappitelli et al., 2014; Costerton et al., 1987; Lewandowski and Beyenal, 2013). Concerning industrial food equipment, the accumulation of unwanted biofilms can result in significant economic losses and in the decreased quality and safety of processed foods (Marchand et al., 2012). Specifically, bacterial biofilms on food contact surfaces of processing equipment may lead to the spoilage of processed products, contamination of product by spoilage bacteria, metal biocorrosion in pipelines and tanks; and reduced heat transfer efficacy in processing equipment (Cappitelli et al., 2014). Therefore, bacterial attachment in food processing environments increases the possibilities of microbial contamination of the processed product (Chmielewski and Frank, 2003).

Psychrotolerant sporeformers, *Bacillus* and *Paenibacillus* genera, are known spoilage bacteria that adhere to production lines and contaminate pasteurized refrigerated foods, e.g., milk (Marchand et al., 2012; de Jonghe et al., 2010). Additionally, it was found that *Bacillus* spp. and *Paenibacillus* spp. are responsible for spoilage of dairy products that had been contaminated by Gram-positive bacteria. Moreover, Gram-positive endospore-forming *Bacillus subtilis* and *Paenibacillus polymyxa* have been isolated from both farm and processing plant environments, and raw and pasteurized fluid milk. *B. subtilis* is not categorized as a human pathogen, however, it has been reported that *B. subtilis* was involved in food poisoning cases. *B. subtilis* induces defects in flavor and texture of yoghurt that are caused due to proteinase activities of *B. subtilis* (Gopal et al., 2015). *P. polymyxa* produces a variety of hydrolytic extracellular enzymes such as proteases, lipases, and lecithinases that can cause the spoilage of pasteurized milk even in the absence of fast bacterial growth. Particularly, the lecithinase activity of *P. polymyxa* is responsible for so-called bitty cream defects in milk due to the aggregation of fat globules (de Jonghe et al., 2010). It has been also reported that *Pseudomonas* spp. can negatively contribute to the quality and shelf life of food due to their ability to form biofilms at low temperatures (Hood and Zottola, 1997; Sørhaug and Stepaniak, 1997).

* Corresponding author at: TUM School of Life Sciences Weihenstephan, Technical University of Munich, Freising, Germany.
E-mail address: olga.fysun@bosch.com (O. Fysun).
[1] Robert Bosch GmbH, Reutlingen, Germany.
[2] Present address: Roche Diagnostics GmbH, Penzberg, Germany.
[3] Present address: Roche Diagnostics GmbH, Mannheim, Germany.

https://doi.org/10.1016/j.mimet.2019.04.015
Received 21 September 2018; Received in revised form 20 April 2019; Accepted 22 April 2019
Available online 22 April 2019

Also, the enhanced attachment of *Listeria monocytogenes* to glass surfaces was observed, which was attributed to the EPS (extracellular polymeric substance) production of *Pseudomonas fragi* (Sasahara and Zottola, 1993).

The fast detection of biofilms is of great importance for the effective prevention of contamination (Cappitelli et al., 2014). Several techniques based on biological, physical, and chemical principles have been employed for the detection of bacterial attachment (Kim et al., 2012a, 2012b; Kirkland et al., 2015; Kwak et al., 2014; Crattelet et al., 2013). However, many of the methods used in the food industry are time-consuming, costly and require trained specialists. Additionally, it has been reported that electrochemical methods can be used for real time detection at early stages of bacterial attachment (Giao et al., 2003). As opposed to the other methods, electrochemical detection has several advantages: data can be processed rapidly, relatively simple and inexpensive instrumentation may be used, and the practical analysis is flexible (Kang et al., 2012; Ahmed et al., 2014).

In electrochemical methods, the reaction under investigation would generate one of the following measurable responses: current, potential or changes in the conductive properties of a medium between electrodes (Moretto and Kalcher, 2014; Zoski, 2007). Voltammetric methods belong to the electrochemical techniques involving the change of the potential at a working electrode versus a reference electrode, while measuring the corresponding current (Armstrong et al., 2000). The reaction of interest, such as the reduction or oxidation of redox couples, occurs on the working electrode. The materials used for the electrodes should be chemically stable and must not interact with any of the species in solution, e.g. platinum or gold are preferred. Also, the miniaturization of the electrodes is a common trend in electrochemistry over the last decades (Ahmed et al., 2014). Cyclic voltammetry (CV) is one of the most used voltammetric methods. This method has been used for monitoring of bacterial attachment on electrochemical microelectrodes (Giao et al., 2003; Harnisch and Freguia, 2012; Becerro et al., 2016).

Several theories have been proposed for the mechanisms of electrochemical detection of bacteria (Nealson and Finkel, 2011; Sultana et al., 2015). According to the literature, the electron transfer can occur: (1) directly to the acceptor via outer membrane cytochromes, or through (2) electron shuttles (redox mediators), (3) conductive nanowires, or (4) other extracellular matrices. Such mechanisms may vary depending on the strain of the microorganism and environmental conditions (Nealson and Finkel, 2011). Although there is not a widely accepted explanation, it is evident that bacteria living in surface-attached biofilms must maintain electrochemical gradients to support basic cellular functions. Usually, electrons are delivered and accepted by dissolved substances. As an examples, some molecules in bacterial biofilms (exoenzymes, exopolysaccharides) adsorbed on the surface of electrodes are believed to catalyze oxygen reduction (Liengen et al., 2014; Faimali et al., 2011).

To the best of our knowledge, despite the numerous studies related to electrochemical detection of bacteria, *B. subtilis* ssp. *subtilis, P. polymyxa, P. fragi* that are known to cause food spoilage, have not yet been studied using electrochemical methods. In addition, there are a few reports only of electrochemical sensors based on interdigitated electrochemical microelectrodes for the detection of bacterial adhesion. Therefore, the aim of this work was to investigate the *B. subtilis* ssp. *subtilis, P. polymyxa, P. fragi* biofilm formation by cyclic voltammetry using interdigitated platinum microelectrodes.

2. Material and methods

2.1. Chemicals

Meat extract and ethanol 70% were supplied by VWR (Darmstadt, Germany). Peptone from casein (pancreatic digest) was obtained from Applichem Panreac (Barcelona, Spain). Plate count agar, and potassium chloride 3 mol L^{-1} were purchased from Merck (Darmstadt, Germany). Potassium ferrocyanide (1%) was obtained from Clin-Tech (Guildford, UK). Freeze-dried cultures of *Bacillus subtilis* ssp. *subtilis* (DSM 10), *Paenibacillus polymyxa* (DSM 36), *Pseudomonas fragi* (DSM 3456) were acquired from DSMZ (Braunschweig, Germany). All the reagents and chemicals were of analytical grade.

2.2. Sample preparation and experimental setup

The freeze-dried cultures of *B. subtilis* ssp. *subtilis* (DSM 10), *P. polymyxa* (DSM 36), *P. fragi* (DSM 3456) were reactivated according to the manufacturer's instructions. A glass ampoule containing the freeze-dried bacteria was cracked by flaming the end and placing three drops of water on the glass. After the cotton plug was removed, 0.5 mL of sterile nutrient medium (5.0 g L^{-1} soya peptone, 3.0 g L^{-1} meat extract) was added. The pellet of freeze-dried bacteria was allowed to rehydrate for 30 min and the contents were mixed using a sterile inoculation loop. Then, 10 μL of the content were added to agar plates, spread with a sterile glass spreader on the surface of the agar, and incubated at 30 °C (*B. subtilis* ssp. *subtilis*, *P. polymyxa*) and at 26 °C (*P. fragi*) for 24 h (DSMZ GmbH, n.d). These agar plate cultures were used for the preparation of a bacterial suspension. A colony was taken from the plate and resuspended in an Eppendorf tube filled with 1 mL of the sterile nutrient medium. The inoculated medium was then transferred into an Erlenmeyer flask with 49 mL of the sterile nutrient medium. The suspension was incubated under stirring at 130 rpm and 30 °C (*B. subtilis* ssp. *subtilis*, *P. polymyxa*) or 26 °C (*P. fragi*) for 2 h until the early log phase of growth. The log phase was detected by measuring the transmission. The optical transmittance at 570 nm of the bacterial suspension at the early log phase was 90.0 ± 3.0%. The number of bacteria in the early log phase corresponds to about 10^6 CFU mL^{-1}. To achieve the bacterial adhesion on the microelectrode surface, a microelectrode was placed into each well of the sterile 6-well plates. Then, the wells were filled with 5 mL of sterile nutrient medium and inoculated with 100 μL of the bacterial suspension at the early log phase as described above. The cleaned and activated microelectrodes were immersed in the wells filled with either sterile nutrient medium or inoculated nutrient medium. The 6-well plates with the microelectrodes were incubated at 30 °C (*B. subtilis* ssp. *subtilis*, *P. polymyxa*) or 26 °C (*P. fragi*) for 18 h.

2.3. Electrochemical methods

The experimental setup has been checked using 100 mM potassium ferrocyanide solution. Platinum interdigitated ring array (IDRA) microelectrodes (MicruX Fluidic, Spain) were cleaned and activated electrochemically before every use. First, they were immersed in ethanol 70% for 5 min. The solvent was then removed with Kimtech Science™ wipes. Secondly, they were rinsed twice with sterile deionized water. After these cleaning steps, the microelectrodes were activated electrochemically using 20 μL of 0.1 M KCl via cyclic voltammetry using a PalmSens 3 bipotentiostat (PalmSens BV, Netherlands) run by a Windows 7 based PC. The potential was cycled 10 times between −1.5 and 1.5 V at a scan rate of 0.100 V s^{-1}. Once the activation step was completed, the microelectrodes were rinsed again twice with sterile deionized water. The electrochemical cell of the microelectrode has a diameter of 2.0 mm. The working electrode has 12 ft pairs. Each foot was 10 μm wide with a 10 μm gap between each foot. The electrochemical cell had a reference electrode, an auxiliary electrode, and two working electrodes. The software PSTrace 4.8 (PalmSens BV, Netherlands) was used to record the data and to control the bipotentiostat. The bipotentiostat was connected to a drop cell (MicruX Fluidic, Spain). For the measurements, the microelectrodes were placed into the slot of the drop cell. Then, 10 μL of either sterile nutrient medium or bacterial suspension of the corresponding well were pipetted onto the electrode surface before the cyclic voltammetry took place. In cyclic voltammetry (CV) a triangular shape potential scan is

applied to an electrode while the current is monitored. A potential scan is performed between two vertex potentials, E_{vtx1} and E_{vtx2}. The potential change is reversed once a vertex potential is reached. For each microelectrode, the cycles were done with the following parameters: $T_{equilibrium} = 15\,s$, $E_{vtx1} = -0.8\,V$, $E_{vtx2} = 0.8\,V$, $E_{step} = 0.01\,V$, scan rate = 50, 100, 250, 350 mV s^{-1}. All the experiments were carried out in ninefold. One scan was conducted for each prepared microelectrode.

2.4. Microscopy

After cyclic voltammetry measurements, the surface of the microelectrodes covered with bacteria biofilm was visualized. The transmitted light microscope (Kern OBN 135, Kern & Sohn GmbH, Germany) was used to visualize the surface of the microelectrodes covered by bacteria. The microelectrodes with biofilms were observed at magnifications of 20× without oil after 10 min of drying at room temperature.

3. Results and discussion

3.1. Electrochemical investigation of Bacillus subtilis ssp. subtilis

Fig. 1 depicts the cyclic voltammogram obtained on the platinum interdigitated microelectrodes for the sterile nutrient medium, the nutrient medium inoculated for 18 h with *B. subtilis* ssp. *subtilis*, and *B. subtilis* ssp. *subtilis* biofilm at scan rate of 250 mV s^{-1}.

As shown in Fig. 1, the presence of *B. subtilis* ssp. *subtilis* biofilm 18 h leads to the pronounced changes in cathodic and anodic current in potential window from −0.2 to −0.8 V. Compared to the *B. subtilis* ssp. *subtilis* biofilm, the difference between nutrient medium and *B. subtilis* ssp. *subtilis* bacterial suspension (planktonic state) at scan rate of 250 mV s^{-1} was not remarkable. Thus, the comparison between nutrient medium and *B. subtilis* ssp. *subtilis* bacterial suspension at different scan rates is required to obtain more details.

Fig. 2 illustrates the anodic (IpA) and cathodic (IpC) peak currents and respective peak potentials (V) obtained from the cyclic voltammogams for the sterile nutrient medium and the nutrient medium inoculated for 18 h with *B. subtilis* ssp. *subtilis,* and *B. subtilis* ssp. *subtilis* biofilm at scan rates of 50, 100, 250 and 350 mV s^{-1}.

The anodic (IpA) and cathodic (IpC) peak currents shown on Fig. 2(A and B) illustrate that the current signals of anodic (oxidation) and cathodic (reduction) curves increase with an increasing scan rate for both nutrient medium and *B. subtilis* ssp. *subtilis* suspension (planktonic state). The current values are slightly increased for *B. subtilis* ssp. *subtilis* suspension when comparing with nutrient medium at the same scan rate. The potential of the anodic peaks (Fig. 2C) does not change with the increasing scan rate. The potential of the cathodic peaks (Fig. 2D) for the *B. subtilis* ssp. *subtilis* suspension slightly shifts towards positive potentials with the increasing scan rate.

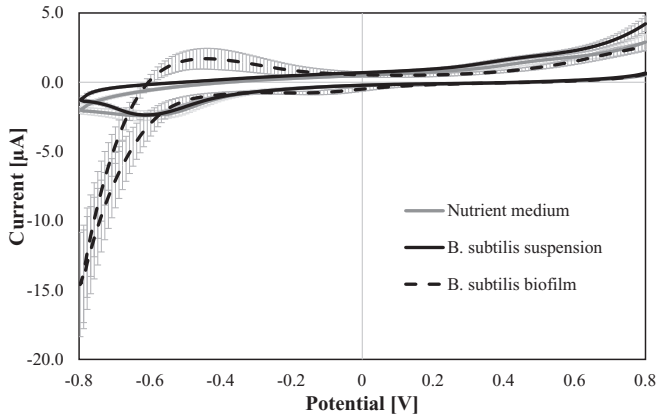

Fig. 1. Cyclic voltammogams obtained for (1) sterile nutrient medium, (2) *B. subtilis* ssp. *subtilis* bacterial suspension 18 h, and (3) *B. subtilis* ssp. *subtilis* biofilm 18 h covering the microelectrode and *B. subtilis* ssp. *subtilis* bacterial suspension 18 h at scan rate of 250 mV s^{-1}. Error bars correspond to the standard errors ($i = 3$, $n = 9$).

3.2. Electrochemical investigation of Paenibacillus polymyxa

Fig. 3 depicts the cyclic voltammogram obtained on the platinum interdigitated microelectrodes for the sterile nutrient medium, the nutrient medium inoculated for 18 h with *P. polymyxa,* and *P. polymyxa* biofilm at scan rate of 250 mV s^{-1}, respectively.

Similarly to Fig. 1, *P. polymyxa* biofilm leads to the pronounced changes in cathodic and anodic current in negative potential window from −0.4 to −0.8 V. Moreover, differences in shape of cyclic voltammorgam are also observed in positive potential window. As shown in Fig. 3, the standard errors of the measurements of the sterile nutrient medium and *P. polymyxa* bacterial suspension 18 h is smaller than that of the measurements of microelectrodes covered with biofilm. Similar behavior can be also observed for *B. subtilis* ssp. *subtilis* (Fig. 1).

Some studies reported large variations in the peak current after bacteria attachment to the surface (Xu et al., 2012; Strycharz et al., 2011; Becerro et al., 2015). The inhomogeneous surface coverage depicted in Fig. 7C may explain the large standard errors.

Fig. 4 illustrate the anodic (IpA) and cathodic (IpC) peak currents and respective peak potentials (V) obtained from the cyclic voltammogams for the sterile nutrient medium and the nutrient medium inoculated for 18 h with *P. polymyxa,* and *P. polymyxa* biofilm at scan rates of 50, 100, 250 and 350 mV s^{-1}.

The anodic (IpA) and cathodic (IpC) peak currents shown on Fig. 4(A and B) illustrate that the current signals of anodic (oxidation) and cathodic (reduction) curves increase with an increasing scan rate for both nutrient medium and *P. polymyxa* suspension 18 h (planktonic state). No remarkable differences have been observed between nutrient medium and *P. polymyxa* suspension 18 h at each scan rate. Similarly to results for *B. subtilis* ssp. *subtilis* suspension (Fig. 2D), cathodic peak slightly shifted towards negative potentials with increasing scan rate for *P. polymyxa* suspension (Fig. 4D). For the anodic peak currents (Fig. 4C), the differences were less pronounced than for the cathodic peaks and no potential shift was observed.

3.3. Electrochemical investigation of Pseudomonas fragi

Fig. 5 depicts the cyclic voltammogram obtained on the platinum interdigitated microelectrodes for the sterile nutrient medium, the nutrient medium inoculated for 18 h with *P. fragi,* and *P. fragi* biofilm 18 h at scan rate of 250 mV s^{-1}, respectively.

Similarly to Figs. 1 and 3, *P. fragi* biofilm formation leads to the pronounced changes in cathodic and anodic current in negative potential window from −0.4 to −0.8 V. Moreover, remarkable differences in shape of cyclic voltammorgam for *P. fragi* suspension (planktonic state) can be observed in positive potential window for the anodic curve. In contrast to Fig. 1 (*B. subtilis* ssp. *subtilis*) and Fig. 3 (*P. polymyxa*), the differences between nutrient medium and bacterial suspension are evident showing higher current values at IpC for *P. fragi* suspension.

The anodic (IpA) and cathodic (IpC) peak currents shown on Fig. 6(A and B) illustrate that the current in anodic (oxidation) and cathodic (reduction) curves increase with an increasing scan rate for both nutrient medium and *P. fragi* suspension 18 h (planktonic state). Moreover, pronounced differences in current at both anodic (IpA) and cathodic (IpC) peak have been observed between nutrient medium and *P. fragi* suspension at each scan rate. *P. fragi* suspension demonstrates higher current values compared to the nutrient medium. It might be contributed to the enhanced electrochemical activity of *P. fragi.* Cathodic peak slightly shifts towards negative potentials with increasing scan rate for the *P. fragi* suspension (Fig. 6C), while potentials

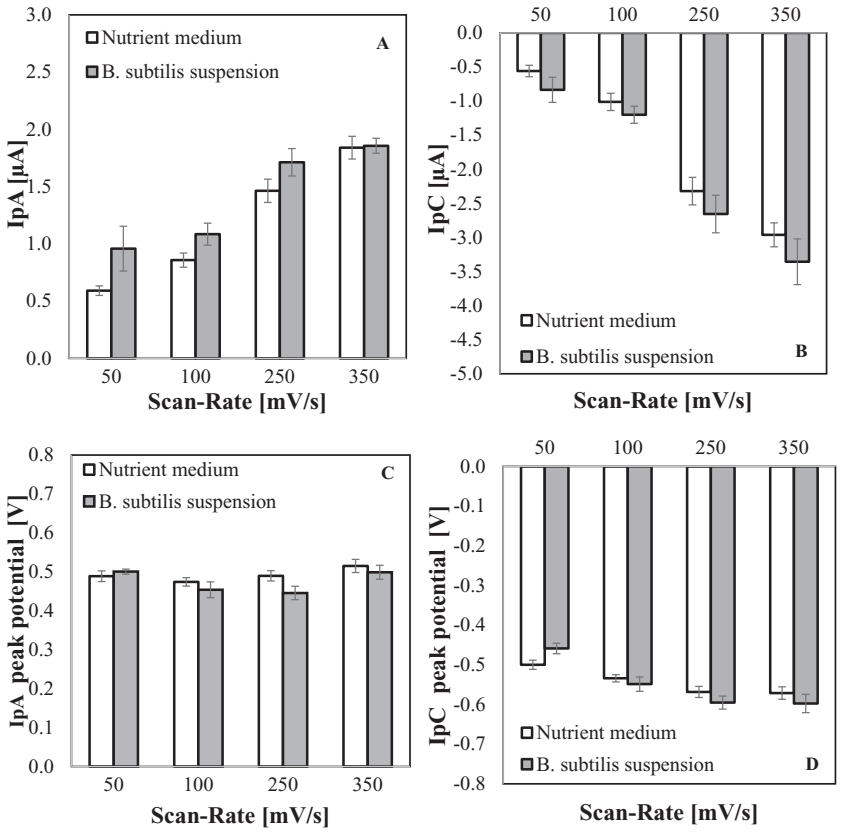

Fig. 2. Anodic (IpA) (A) and cathodic (IpC) (B) peak currents and respective peak potentials (V) (C and D, respectively) for nutrient medium and *B. subtilis* ssp. *subtilis* suspension 18 h obtained at scan rates of 50, 100, 250 and 350 mV s^{-1}. Error bars correspond to the standard errors ($i = 3$, $n = 9$).

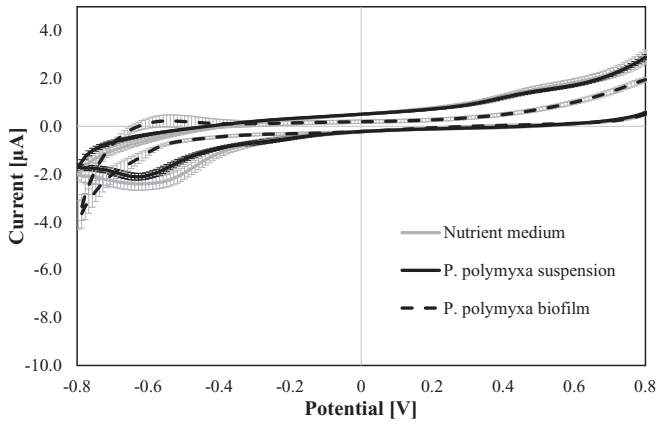

Fig. 3. Cyclic voltammogams obtained for (1) sterile nutrient medium, (2) *P. polymyxa* bacterial suspension 18 h, and (3) *P. polymyxa* biofilm 18 h covering the microelectrode and *P. polymyxa* bacterial suspension 18 h at scan rate of 250 mV s^{-1}. Error bars correspond to the standard errors ($i = 3$, $n = 9$).

at anodic peaks do not shifted notably (Fig. 6D).

3.4. Microscopy

A detailed visualization of the *B. subtilis* ssp. *subtilis, P. polymyxa, P. fragi* adhesion on the surface of microelectrodes was obtained using transmitted light microscopy (Fig. 7).

Fig. 7A shows the clean interdigitated microelectrode with pairs of feet of the IDRA structure. Fig. 7B–D depict the attachment of bacteria to the working electrode after 18 h of incubation in nutrient medium. The bacterial distribution on the surface is non-homogeneous, showing bacterial communities in clusters and single cells. Non-homogeneous bacterial biofilm formation may explain the deviations in the voltammetric measurements using microelectrodes. The partial removal of the bacteria from the working electrode surface was observed after three CV cycles. The removal of adhered bacteria may result from the formation of bubbles, which occurred at large positive and negative potentials, thus, leading to the mechanical removal of bacteria. Bacteria removal during cyclic voltammetry, especially at low scan rates of 0.150 V s^{-1}, has been observed previously by Giao et al., 2003. In the study of Giao et al., 2003 it was reported that most of the bacteria remaining on the surface were viable. At higher scan rates (0.500 V s^{-1}) the number of dead bacteria on the surface increased (Giao et al., 2003). Thus, the parameters of cyclic voltammetry must be selected carefully to prevent the removal or death of the adhered bacteria.

3.5. Electrochemical microsensors for detection of bacterial adhesion

Previous research has documented the applicability of cyclic voltammetry for the bacteria detection (Marsili et al., 2008; Giao et al., 2003; Becerro et al., 2016). In this work, cyclic voltammetry (CV) was investigated to detect the bacterial biofilms using interdigitated platinum microelectrodes.

Vieira et al., 2003 studied bacterial detection using cyclic voltammetry with platinum microelectrodes. It was reported that the shape of the cyclic voltammogram may provide information on the surface coverage. According to the authors, as the coverage of the surface increases, the peaks' intensity in the voltammograms will decrease. The author's explanation is based on the fact that as the accumulation on the surface increases, the area available for the oxidation-reduction processes decreases. Becerro and collaborators (Becerro et al., 2016) evaluated the cyclic voltammetry and differential pulse voltammetry for detection of *Staphylococcus epidermidis*. At the beginning of the

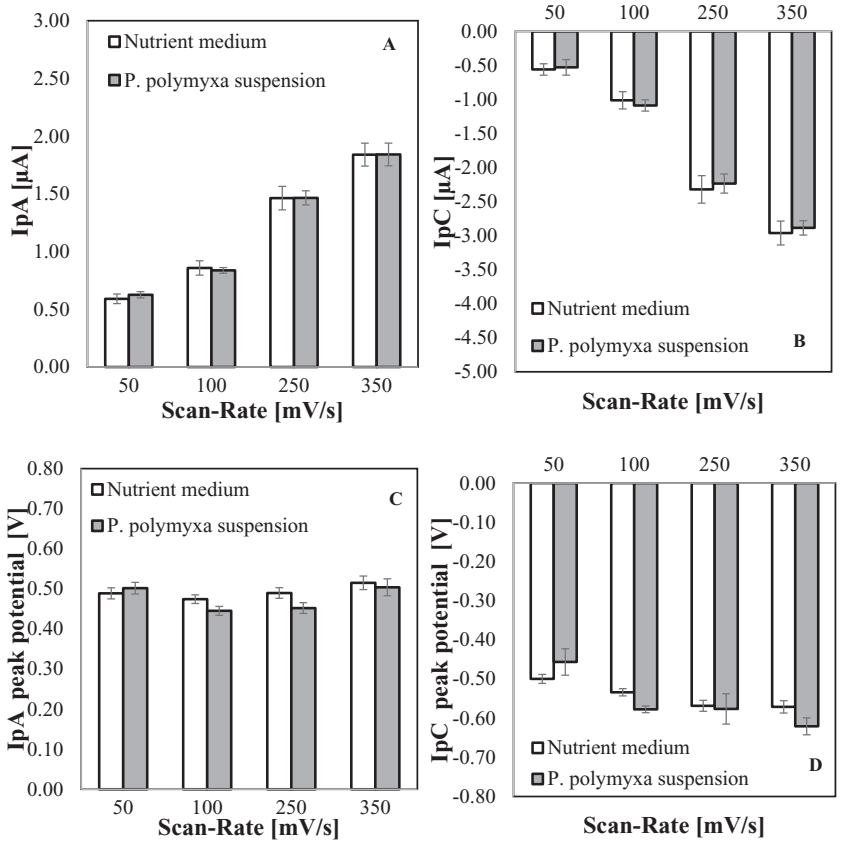

Fig. 4. Anodic (IpA) (A) and cathodic (IpC) (B) peak currents and respective peak potentials (V) (C and D, respectively) for nutrient medium and *P. polymyxa* suspension 18 h obtained at scan rates of 50, 100, 250 and 350 mV s^{-1}. Error bars correspond to the standard errors (i = 3, n = 9).

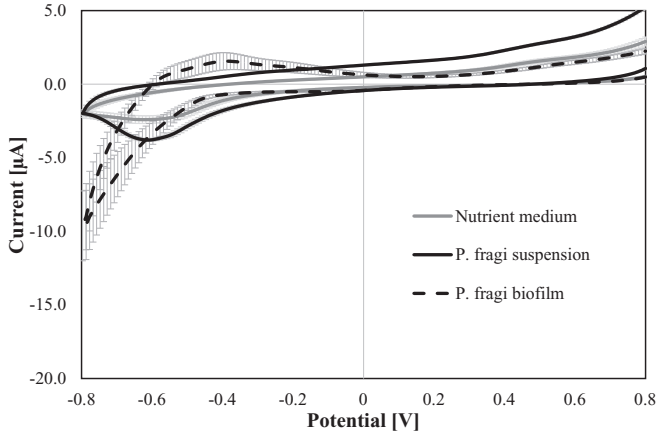

Fig. 5. Cyclic voltammogams obtained for (1) sterile nutrient medium, (2) *P. fragi* bacterial suspension 18 h, and (3) *P. fragi* biofilm 18 h covering the microelectrode and *P. fragi* bacterial suspension 18 h at scan rate of 250 mV s^{-1}. Error bars correspond to the standard errors (i = 3, n = 9).

experiment, they recorded the oxidation and reduction peaks and observed an increase in the current value. These peaks may be indicative of the bacterial growth. Once the biofilm developed completely, they observed a decrease in current that may be caused by enzymatic activity of bacteria. The voltammograms were correlated with the activity of different redox centers present on the bacterial surface that are related to the metabolic activity of bacterial cells (Becerro et al., 2016). Also in present work, it may be assumed that metabolic activity of selected bacteria contributes to the current increases which were showed in cyclic voltammograms (Figs. 1, 3, and 5). A possible explanation for the increased peak currents is an enhanced electron transfer between bacteria and the electrode surface. According to Nealson et al. (Nealson and Finkel, 2011), electrochemical reactions during cyclic voltammetry can occur for all bacterial products, e.g., secreted exoenzymes, carbohydrates, and exopolysaccharides (EPS). It can be assumed that since *B. subtilis* ssp. *subtilis*, *P. polymyxa*, *P. fragi* can produce a variety of enzymes including, proteases and lipases and produce EPS, they may interfere with electron transport.

Marsili et al., 2008 studied the effect of low scan rates on the results of cyclic voltammetry measurements to understand the main redox-active species that participate in the electron transfer processes to an electrode from *Geobacter sulfurreducens*. As the scan rate decreases, the kinetic effects of electron transfer between cell surface and the electrodes were minimized, and the enzymatic effects, which are related to bacterial activity, became primary factors. As the scan rate increased, slow reactions may not have time to occur before the potential was changed to the next step. Thus, the kinetics of interfacial electron transfer between redox proteins and electrodes strongly affects the voltammetric response and the kinetics of continuous enzymatic turnover may be masked.

According to literature, the use of microelectrode systems offers several advantages compared to macroelectrodes: higher sensitivities, enhanced mass transport, better signal-to-noise ratio and no need for supporting electrolyte (Becerro et al., 2016; Garci-A-Aljaro et al., 2010). It has also been reported that the signal measured for the attached bacteria is more significant for microelectrodes with smaller active surface area (Laczka et al., 2008). Moreover, the design and features of interdigitated microelectrode arrays eliminate the need for a reference electrode, allowing for a simpler experimental setting than in classical three or four electrode systems. In addition, IDA electrodes with small gap between microbands may provide better sensitivity for bacteria

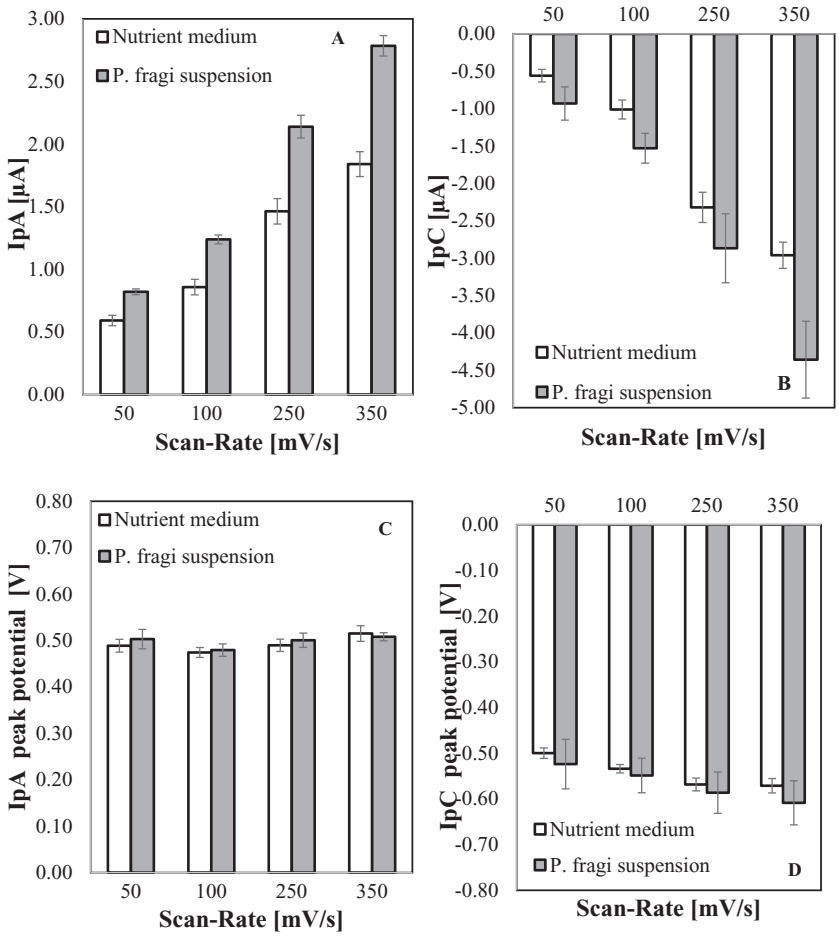

Fig. 6. Anodic (IpA) (A) and cathodic (IpC) (B) peak currents and respective peak potentials (V) (C and D, respectively) for nutrient medium and *P. fragi* suspension 18 h obtained at scan rates of 50, 100, 250 and 350 mV s^{-1}. Error bars correspond to the standard errors (i = 3, n = 9).

detection (Kim et al., 2012a, 2012b). The configuration for the interdigitated array microelectrodes is the paired electrode configuration (generation/collection scheme). The intermediate species generated on one electrode (generator), diffuses to the other electrode (collector), where it can be regenerated to the initial reactant present in bulk solution (Zoski, 2007). The interdigitated electrodes of smaller features show significantly higher perimeters and smaller surface areas than single electrodes occupying a similar pattern. It has been demonstrated that the perturbation produced by the binding of big targets, such as bacteria, is more significant for electrodes of smaller active surface area (Laczka et al., 2008).

When it comes to the processing equipment, an important aspect is the comparability between the electrode material and the material of contact surfaces in processing equipment. Platinum is a metal commonly used as an electrode material. However, platinum is not used material in industrial equipment for contact surfaces. Therefore, it is important to compare its surface properties to the most commonly used material in processing equipment, e.g., stainless steel. Important surface properties are the adhesion free energy and the hydrophobicity of both materials (Teixeira and Oliveira, 1999). From the results published in the literature, it can be seen that the difference between them is rather negligible. The adhesion free energy for platinum is 43.98 mJ m^{-2}, while for stainless steel 42.35 mJ m^{-2}. The hydrophobicity for platinum was defined as 53.02 mJ m^{-2}, while for stainless steel 45.21 mJ m^{-2} (Teixeira and Oliveira, 1999). Thus, it can assumed that the initial bacterial attachment should be nearly similar on both materials.

Accordingly, both electrochemical sensors and biosensors can be used for bacterial detection (Grieshaber et al., 2008; Ahmed et al., 2014). Sensors are devices with a receptor specific for an analyte (molecular or ionic recognition). The response detected by the receptor is converted into an electric signal by the transducer. Electrochemical biosensors are based on the same principles as electrochemical sensors are. However, electrochemical biosensors are differentiated from electrochemical sensors according to the biorecognition element used as receptor: enzymes, nucleic acids, aptamers, antibodies, organelles, membranes, cells, tissues, or even whole organisms (Moretto and Kalcher, 2014). Thus, electrochemical biosensors for bacterial detection require receptors such as enzymes, antibodies, phages, or DNA. Several publications in recent years report whole-cell bacterial detection using electrochemical biosensors (Ahmed et al., 2014; Vanegas et al., 2016). However, due to the protein nature, biorecognition elements in biosensors are not stable at high temperatures (above 80 °C) or common pressures, or in the presence of steam and under typical machine cleaning conditions (acidic and basic solutions) (Moretto and Kalcher, 2014). Thus, electrochemical biosensors cannot be implemented in industrial processing equipment for long term usage. Electrochemical biosensors can be recommended for the quality control in laboratories, while electrochemical sensors without a biorecognition element can be potentially implemented into processing equipment for the monitoring of bacterial biofilms. Nevertheless, it should be noted that the major drawback of the electrochemical sensors is that every bacteria type cannot be identified with this technique. Although the remarkable differences in cyclic voltammograms between *B. subtilis* ssp. *subtilis, P. polymyxa, P. fragi* biofilms have been shown in this study, it is assumed that only real time biofilm detection without bacteria identification

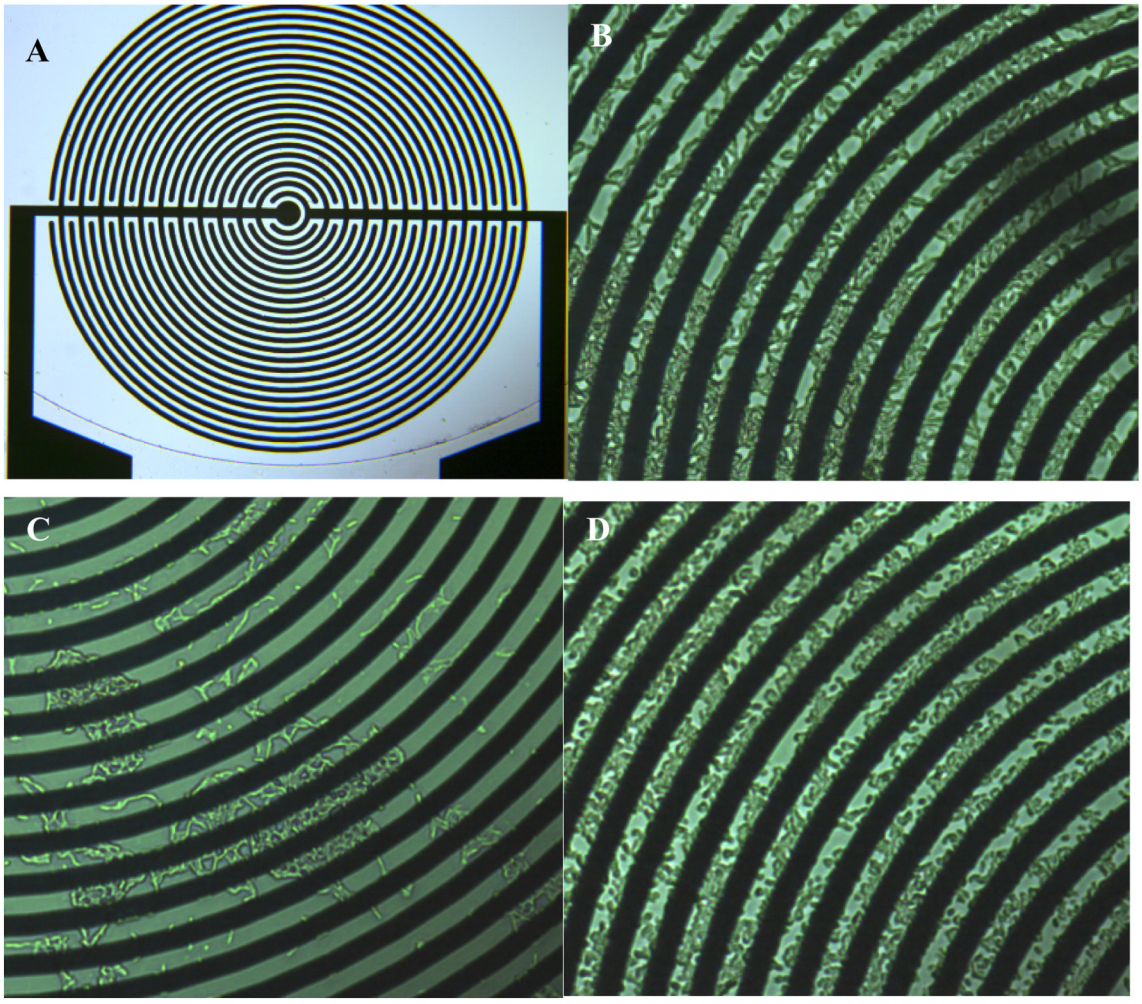

Fig. 7. Surface of clean interdigitated ring array (IDRA) microelectrode (A) and microelectrodes with (B) *B. subtilis* ssp. *subtilis* biofilm, (C) *P. polymyxa* biofilm, (D) *P. fragi* biofilm (after 18 h incubation in nutrient medium).

might be possible in processing equipment.

4. Conclusion

The results from this study indicate that the electrochemical detection of *B. subtilis* ssp. *subtilis, P. polymyxa, P. fragi* biofilms on surfaces with interdigitated ring array platinum microelectrodes is possible. The results from cyclic voltammograms obtained at scan rates of 50, 100, 250 and 350 mV s^{-1} showed that a current increase was observed after bacterial attachment to the microelectrode surfaces. Further studies are being performed to detect bacterial attachment on electrodes in flow conditions. In addition, improvement of the electrochemical microsensors for better sensitivity and their adaptation under production conditions for real time detection will be investigated in the near future.

Acknowledgments

This research did not receive any specific grant from funding agencies in the public, commercial, or not-for-profit sectors.

References

Ahmed, A., Rushworth, J.V., Hirst, N.A., Millner, P.A., 2014. Biosensors for whole-cell bacterial detection. Clin. Microbiol. Rev. 27 (3), 631–646. https://doi.org/10.1128/CMR.00120-13.

Armstrong, F.A., Camba, R., Heering, H.A., Hirst, J., Jeuken, L.J.C., Jones, A.K., Leger, C., McEvoy, J.P., 2000. Fast voltammetric studies of the kinetics and energetics of coupled electron-transfer reactions in proteins. Faraday Disc 116, 191–203. https://doi.org/10.1039/b002290j.

Becerro, S., Paredes, J., Arana, S., 2015. Multiparametric biosensor for detection and monitoring of bacterial biofilm adhesion and growth. In: Lacković, I., Vasic, D. (Eds.), 6th European Conference of the International Federation for Medical and Biological Engineering. Springer International Publishing, Cham, pp. 333–336.

Becerro, S., Paredes, J., Mujika, M., Lorenzo, E.P., Arana, S., 2016. Electrochemical real-time analysis of bacterial biofilm adhesion and development by means of thin-film biosensors. IEEE Sensors J. 16 (7), 1856–1864. https://doi.org/10.1109/JSEN.2015.2504495.

Cappitelli, F., Polo, A., Villa, F., 2014. Biofilm formation in food processing environments is still poorly understood and controlled. Food Eng. Rev. 6 (1–2), 29–42. https://doi.org/10.1007/s12393-014-9077-8.

Chmielewski, R.A.N., Frank, J.F., 2003. Biofilm formation and control in food processing facilities. Comp Rev Food Sci Food Safety 2 (1), 22–32. https://doi.org/10.1111/j.1541-4337.2003.tb00012.x.

Costerton, J.W., Cheng, K.J., Geesey, G.G., Ladd, T.I., Nickel, J.C., Dasgupta, M., Marrie, T.J., 1987. Bacterial biofilms in nature and disease. Annual Reviews in Microbiology 41 (1), 435–464. https://doi.org/10.1146/annurev.mi.41.100187.002251.

Crattelet, J., Ghnimi, S., Debreyne, P., Zaid, I., Boukabache, A., Esteve, D., Auret, L., Fillaudeau, L., 2013. On-line local thermal pulse analysis sensor to monitor fouling and cleaning: application to dairy product pasteurisation with an ohmic cell jet heater. J. Food Eng. 119 (1), 72–83.

DSMZ GmbH, catalogues - Psuedomonas fragi (Eichholz 1902) Gruber n.d: DSM No.: 3456, available at https://www.dsmz.de/catalogues/details/culture/DSM-3456.html

Faimali, M., Benedetti, A., Pavanello, G., Chelossi, E., Wrubl, F., Mollica, A., 2011. Evidence of enzymatic catalysis of oxygen reduction on stainless steels under marine biofilm. Biofouling 27 (4), 375–384. https://doi.org/10.1080/08927014.2011.576756.

Garci-A-Aljaro, C., Bangar, M.A., Baldrich, E., Munoz, F.J., Mulchandani, A., 2010. Conducting polymer nanowire-based chemiresistive biosensor for the detection of bacterial spores. Biosens. Bioelectron. 25, 2309–2312.

Giao, M.S., Montenegro, M.I., Vieira, M.J., 2003. Monitoring biofilm formation by using cyclic voltammetry-effect of the experimental conditions on biofilm removal and

activity. Water Sci. Technol. 47 (5), 51–56.
Gopal, N., Hill, C., Ross, P.R., Beresford, T.P., Fenelon, M.A., Cotter, P.D., 2015. The prevalence and control of bacillus and related spore-forming bacteria in the dairy industry. Front. Microbiol. 6, 1418. https://doi.org/10.3389/fmicb.2015.01418.
Grieshaber, D., MacKenzie, R., Vörös, J., Reimhult, E., 2008. Electrochemical Biosensors - Sensor Principles and Architectures. vol. 8 MDPI AG, Basel, Switzerland. https://doi.org/10.3390/s80314000.
Harnisch, F., Freguia, S., 2012. A basic tutorial on cyclic voltammetry for the investigation of electroactive microbial biofilms. Chem. Asian J. 7 (3), 466–475. https://doi.org/10.1002/asia.201100740.
Hood, S.K., Zottola, E.A., 1997. Adherence to stainless steel by foodborne microorganisms during growth in model food systems. Int. J. Food Microbiol. 37 (2–3), 145–153. https://doi.org/10.1016/S0168-1605(97)00071-8.
de Jonghe, V., Coorevits, A., de Block, J., van Coillie, E., Grijspeerdt, K., Herman, L., de Vos, P., Heyndrickx, M., 2010. Toxinogenic and spoilage potential of aerobic spore-formers isolated from raw milk. Int. J. Food Microbiol. 136 (3), 318–325. https://doi.org/10.1016/j.ijfoodmicro.2009.11.007.
Kang, J., Kim, T., Tak, Y., Lee, J.-H., Yoon, J., 2012. Cyclic voltammetry for monitoring bacterial attachment and biofilm formation. J. Ind. Eng. Chem. 18 (2), 800–807. https://doi.org/10.1016/j.jiec.2011.10.002.
Kim, Y.W., Sardari, S.E., Meyer, M.T., Iliadis, A.A., Wu, H.C., Bentley, W.E., Ghodssi, R., 2012a. An ALD aluminum oxide passivated surface acoustic wave sensor for early biofilm detection. Sensors Actuators B Chem. 163, 136–145.
Kim, Seonghwan, Yu, Guiduk, Kim, Taeyoung, Shin, Kyusoon, Yoon, Jeyong, 2012b. Rapid bacterial detection with an interdigitated array electrode by electrochemical impedance spectroscopy. Electrochim. Acta 82, 126–131. https://doi.org/10.1016/j.electacta.2012.05.131.
Kirkland, C.M., Herrling, M.P., Hiebert, R., Bender, A.T., Grunewald, E., 2015. In situ detection of subsurface biofilm using low-field NMR: A field study. Environ. Sci. Technol. 49, 11045–11052.
Kwak, Yeon Hwa, Lee, Junhee, Lee, Junghoon, Kwak, Soo Hwan, Oh, Sangwoo, Paek, Se-Hwan, Ha, Un-Hwan, Seo, Sungkyu, 2014. A simple and low-cost biofilm quantification method using LED and CMOS image sensor. J. Microbiol. Methods 107, 150–156. https://doi.org/10.1016/j.mimet.2014.10.004.
Laczka, O., Baldrich, E., Muñoz, F.X., del Campo, F.J., 2008. Detection of Escherichia coli and Salmonella typhimurium using interdigitated microelectrode capacitive immunosensors. The importance of transducer geometry. Anal. Chem. 80 (19), 7239–7247. https://doi.org/10.1021/ac800643k.
Lewandowski, Z., Beyenal, H., 2013. Fundamentals of Biofilm Research. CRC Press/Taylor & Francis Group, Boca Raton.
Liengen, T., Basseguy, R., Feron, D., Beech, I., Birrien, V., 2014. Understanding Biocorrosion: Fundamentals and Applications. Elsevier Reference Monographs (ISBN 978-1-78242-125-2).
Marchand, S., de Block, J., de Jonghe, V., Coorevits, A., Heyndrickx, M., Herman, L., 2012. Biofilm formation in Milk production and processing environments; influence on milk quality and safety. Compr. Rev. Food Sci. Food Saf. 11 (2), 133–147. https://doi.org/10.1111/j.1541-4337.2011.00183.x.
Marsili, E., Baron, D.B., Shikhare, I.D., Coursolle, D., Gralnick, J.A., Bond, D.R., 2008. Shewanella secretes flavins that mediate extracellular electron transfer. Proc. Natl. Acad. Sci. U. S. A. 105 (10), 3968–3973. https://doi.org/10.1073/pnas.0710525105.
Moretto, L.M., Kalcher, K., 2014. Environmental Analysis by Electrochemical Sensors and Biosensors. Springer New York, New York, NY. https://doi.org/10.1007/978-1-4939-0676-5.
Nealson, K.H., Finkel, S.E., 2011. Electron flow and biofilms. MRS Bull. 36 (5), 380–384. https://doi.org/10.1557/mrs.2011.69.
Sasahara, K., Zottola, E., 1993. Biofilm formation by listeria monocytogenes utilizes a primary colonizing microorganism in flowing systems. J. Food Prot. 56 (12), 1022–1028.
Sørhaug, T., Stepaniak, L., 1997. Psychrotrophs and their enzymes in milk and dairy products. Quality aspects. Trends Food Sci. Technol. 8 (2), 35–41. https://doi.org/10.1016/S0924-2244(97)01006-6.
Strycharz, S.M., Malanoski, A.P., Snider, R.M., Yi, H., Lovley, D.R., Tender, L.M., 2011. Application of cyclic voltammetry to investigate enhanced catalytic current generation by biofilm-modified anodes of Geobacter sulfurreducens strain DL1 vs. variant strain KN400. Energy Environ. Sci. 4 (3), 896–913. https://doi.org/10.1039/C0EE00260G.
Sultana, S.T., Babauta, J.T., Beyenal, H., 2015. Electrochemical biofilm control: A review. Biofouling 31 (9–10), 745–758. https://doi.org/10.1080/08927014.2015.1105222.
Teixeira, P., Oliveira, R., 1999. Influence of surface characteristics on the adhesion of alcaligenes denitrificans to polymeric substrates. J. Adhes. Sci. Technol. 13 (11), 1287–1294. https://doi.org/10.1163/156856199X00190.
Vanegas, D.C., Gomes, C., McLamore, E.S., 2016. Biosensors for indirect monitoring of foodborne Bacteria. Biosens J 5 (1). https://doi.org/10.4172/2090-4967.1000137.
Vieira, M.J., Pinho, I.A., Gião, S., Montenegro, M.I., 2003. The use of cyclic voltammetry to detect biofilms formed by pseudomonas fluorescens on platinum electrodes. Biofouling 19 (4), 215–222.
Xu, S., Liu, H., Fan, Y., Schaller, R., Jiao, J., Chaplen, F., 2012. Enhanced performance and mechanism study of microbial electrolysis cells using Fe nanoparticle-decorated anodes. Appl. Microbiol. Biotechnol. 93 (2), 871–880.
Zoski, C.G. (Ed.), 2007. Handbook of Electrochemistry. United Kingdom Elsevier, Oxford.